

The effect of cold rolling on mechanical properties and microstructure of aluminium 6082 T6 joint by friction stir welding process

*Tshepo Gaonnwe*¹, *Madindwa Mashinini*², and *Mothibeli Pita*²

¹Department of Mechanical Engineering, Faculty of Engineering and Technology, University of South Africa, Johannesburg, South Africa
gaont@unisa.ac.za

²Department of Mechanical and Industrial Engineering, Faculty of Engineering and Technology, University of Johannesburg, South Africa
mmashinini@uj.ac.za

²Department of Mechanical Engineering, Faculty of Engineering and Technology, University of South Africa, Johannesburg, South Africa
pitam@unisa.ac.za

Abstract: Cold rolling increases the strain hardening coefficient and improves the material's mechanical strength and formability while maintaining uniform sheet thickness. This paper investigates the effects of cold rolling on the mechanical properties of Aluminum 6082 T6 during the friction stir welding (FSW) process. Aluminum 6082 T6 material was cold rolled to reduce the thickness by 50 percent. Rolled and as-received material were welded by friction stir welding process using the same welding parameters. Welded samples were characterized by optical microscopy. Tensile and hardness tests were conducted on the welded sample. The findings shows a slight difference in tensile strength between rolled and as-received welded sample as it is reported to be 1.7%. Rolled sample was 3.5% more harder on the weld zone than as-received sample.

Key words: FSW, tensile, cold reduction, microstructure

1. Introduction

Bulk materials with a high strength to weight ratio are in high demand these days, especially in weight-critical industrial applications (Ghalehbandi and Malaki, 2019). The conventional light-weight metals including aluminium, magnesium and copper are widely used for structural applications in the automotive, aerospace, and electronics industries, but improvements in the mechanical properties of these metals would be attractive for enhancing their fabrication capabilities (Kawasaki and Langdon, 2018). Al-Mg-Si alloys within situ Mg₂Si reinforcing particles are attractive candidate materials for aerospace, automotive and other applications (Zhu et al., 2019). The strength of these alloys are enhanced by strain hardening or cold-working which is accomplished by cold rolling, drawing and other similar operations where area reduction is obtained during forming process (Baruah and Borah, 2020). Severe plastic deformation (SPD) was developed by Russian scientists as a new method of manufacturing bulk specimens having ultrafine grained (UFG) microstructure (Kim et

al., 2004). There are many SPD techniques like ARB (Accumulative Roll Bonding), ECAP (Equal channel angular pressing) and HPT (High pressure tension) to produce UFG metallic materials (Sun et al., 2009). The structural changes caused by SPD are reflected in improved mechanical properties such as tensile strength and hardness (Kurzydłowski, 2004). In structural applications, a material's mechanical properties plays a significant role (Pita & Mashinini, 2020). Heavy deformations by cold rolling or drawing, can result in significant refinement of microstructure at low temperatures (Valiev, Islamgaliev & Alexandrov, 2000). It has a significant effect on the mechanical properties of alloys, and predictions can be made concerning the properties if the amount of cold work is known (Ortiz et al., 2007). Friction stir welding (FSW) was invented as a solid-state welding process in 1991 and has become widespread worldwide due to its advantages over traditional joining methods (Nginda and Pita, 2022). The severe plastic deformation and high temperature exposure within the stirred zone during friction stir welding (FSW) result in dynamic recrystallization (DRX) and microstructure evolution, which determines the final grain structure and the performance of weld joints (Yu, Wu and Shi, 2021). The grain size which is influenced by heat generated during FSW results in reduction of mechanical properties and formability of welds caused by thermal cycles (Tejonadha Babu, Muthukumaran and Bharat Kumar, 2018). Depending on the amount of heat input during welding, the magnitude of the (Heat affected zone) HAZ increases or decreases as temperature of the material increases or decreases (Cueca et al., 2012). Heavy deformations, for example, by cold rolling or drawing, can result in significant refinement of microstructure at low temperatures (Valiev, Islamgaliev and Alexandrov, 2000). Cold work reduction of metals and alloys causes an increase in dislocation density with a build-up of internal energy and this internal energy can be displayed through the increase in the metal tensile properties—ultimate tensile strength (UTS) and yield strength (YS) (Qassab and Qassab, 2017). During FSW, different locations across the joint are subjected to different thermal cycles, potentially leading to a wide range of precipitate microstructure since the thermal stability of these precipitates is low, correspondingly resulting in different hardening behaviour and exhibiting diverse hardness (Dong et al., 2013). Increasing of rotational speed, and axial load lead to increasing the hardness value in stirring zone due to the mixing between the two plates in it (M. S. Mahany, Reham Reda Abbas, M.M.Z. Ahmed, 2017).

Cold rolling increases the strain hardening coefficient and enhances the mechanical strength and formability of the material while maintaining uniform sheet thickness (Behaviour et al., 2020). Although grain growth can occur during or after recrystallization of material that has been subjected to a small critical amount of prior cold work (Qassab and Qassab, 2017). Plastic deformation is most effective method to improve the microstructure and mechanical properties of materials (Wang et al., 2021). However, the FSW process has a substantial drawback relating to the low stability of the welded materials against the abnormal grain growth (Kalinenko et al., 2021), and the mechanical properties are seriously diminished by the effect of heat introduced by the welding process (Cueca et al., 2012). This paper investigates the effect of strain hardening material, before the FSW process, on the microstructure and mechanical properties during friction stir welding.

2. Methodology

2.1 Materials

Aluminum 6082 T6 material of 200 mm length ,75 mm width and 12 mm thickness were cold rolled to 6 mm. The same material of the same dimensions but a thickness of 6 mm as-received material was cut accordingly. Three sparks analysis were done per sample by using glow discharge optical emission spectroscopy (GD-OES). The GD-OES was calibrated first by using aluminum metal standard block before analysis. An average was then calculated from the three analysis and the results are tabulated below. Trace elements were filtered from raw data and only major alloying elements for aluminum alloys were reported.

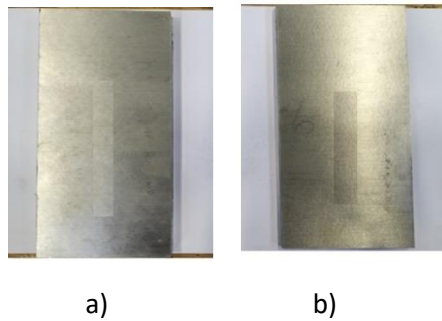


Figure 1 : a) 12 mm thickness as-received b) 6mm thickness as-received

Table 1: Chemical composition base material

Chemical composition								
Element (Wt.%)	Si	Fe	Cu	Mn	Mg	Cr	Zn	Al
Base	1.02	0.306	0.246	0.6	0.74	0.016	0.004	97

2.2 Cold rolling experiment

Al 6082 T651 was cold rolled using a Carl Wezel Muhlacker rolling machine which is presented in figure 2, to reduce the thickness by 50% on first pass. The plate of 200 mm length,75 mm width, and 12 mm thickness plate were rolled to 6 mm on first pass. The rolling speed was set to 12.25 rpm, load applied on the samples was 0,14 tons and rollers space was set to be 6 mm. The material rolled elongated to approximately 360 mm in length with the same width of 75 mm and thickness of 6 mm. The rolling speed was set to 12.25 rpm and the applied load was 0.14 tons, with a roller space of 6 mm.



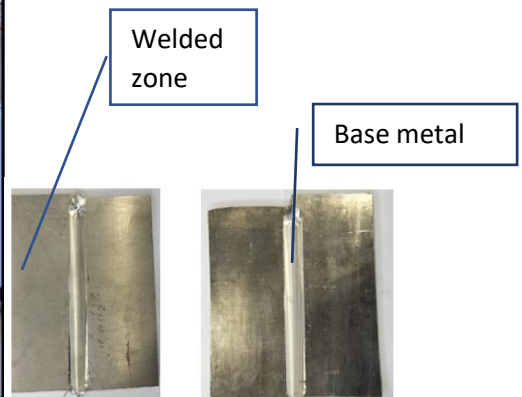
Figure 2 : Carl Wezel rolling machine

2.3 FSW experimentation

As-received and cold-reduced samples were joined by I-Stir (Friction stir welding) FSW machine. The two cold rolled plates and as-received material were firmly clamped on the FSW machine horizontally on top of the backplate to ensure that they are level and not affected by vibration when the tool is rotating at high RPMs. These samples were friction stir welded with 3.5 mm depth threaded tapered cylindrical tool at zero-degree tilt angle with a spindle speed of 550 rpm, feed rate of 300mm/min, and depth of 3.5 mm and downwards axial force of 1kN. The FSW machine was used to join the sample as shown in figure 3 and welded samples are presented in figure 3(b-c).



(a)



(b)

(c)

Figure 3(a-c): a) FSW machine(b) As-received FSW welded (c) Cold rolled FSW welded

2.4 Microstructure

The FSW welded samples were cut perpendicular to the welding zone using a Struers Secotom-60 cutting machine with a high-quality titanium cut-off wheel (20S25). The samples were then mounted using a struers CitoPress-15 mounting press machine. AKA Resin Phenolic SEM black conductive resin was used to mount all samples. The mounted samples were mechanically grounded with a Struers Tegramin-20 grinding and polishing machine. Silicon carbide (SiC) grinding papers with grit sizes of 80, 320, 1200 and 4000, were used for grinding the samples, which were later surface finished by polishing it to a mirror finish using Diapro MD-Mol 3 μ m diamond suspension and colloidal silica 0.04 μ m OP-S suspension for 3min. The specimens were etched with Hatch's reagent, a solution containing 100ml H₂O, and 10 grams NaOH. The metallographically prepared and etched samples were observed for microstructure using a Zeiss crossbeam 340 scanning electron microscope (SEM).

2.5 Tensile test

Tensile test was performed on as-received and rolled welded samples according to ASTM E8/E8M-13a standard. Four samples were machine per category, as shown in figure (4). The tests were conducted using Instron 8801 servo hydraulic fatigue testing system. the following data was obtained and analyzed, modulus of elasticity, 0.2 percent yield strength, maximum load reached by the samples, and percentage elongation, as shown in table 2.



Figure 4(a-b): Tensile test samples of (a) As-received FSW welded (b) Cold rolled FSW welded

Table 2: Tensile test results

Samples	Percentage elongation [%]	Maximum force [kN]	Tensile strength at yield [Mpa]	Modulus [Mpa]
Rolled FSW welded	3,05	5,98	118	80651,5
As-received FSW welded	1,99	5,64	119,99	77552,5

2.6 Hardness test

A hardness test was performed on a sectioned sample of as-received and cold-rolled according to the ASTM E384 standard. The tests were performed on the base metal (BM), heat affect zone (HAZ), and weld zone (WZ). The test was conducted on the HBRV-187.5D digital universal hardness tester presented in figure 5. The test force was 306.5 N with a holding time of 10 seconds. The results obtained from the machine are shown in table 3.

Table 3: Hardness test results

Samples	Welded zone	Heat affected zone	Base metal
Rolled FSW welded	113,4 HV	102,9 HV	154,8 HV
As-received FSW welded	109,4 HV	105,1 HV	137,3 HV



Figure 5: HBRV-187.5D Digital hardness testing machine

3. Results and discussion

Figure 6(a-b) shows the optical microscope images of as- received and cold rolled welded samples on welded zone (WZ), heat affected (HAZ) and base metal (BM). It was noticed that the material had fully recrystallized where the tool was rotating. The weld nugget zone, where plastic deformation and temperature are the highest is characterized by the finest structure, due to the dynamic recrystallisation process(Laska et al., 2022). Homogeneously distributed black spots were noticed on the images of both samples and the one for cold rolled sample were bigger than as-received sample on weld zone. The material might have reacted differently when heat was generated on a weld zone because of the cold rolling effect.

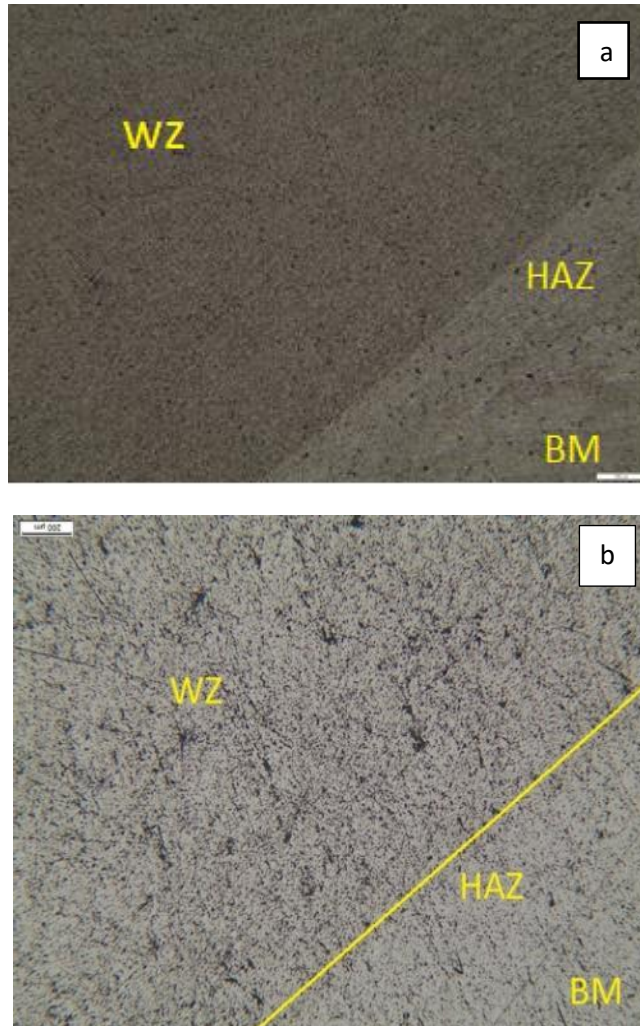


Figure 6: a) Optical microscopy (OM) image of as-received material at 200µm magnification b) OM images of Cold rolled material 200µm.

Figures 7 & 8 present the second phases available on WZ of both materials that might have had an influence on the material thus explaining the mechanical behaviour on a microscopic level. Second phase identified on optical microscope was further investigated on (scanning

electron microscope)SEM. The second phases identified were Mg₂Si shown on both cold rolled and as-received material WZ. Mg₂Si has a low density (1.90 g/cm³), a high melting point (1087 °C), a high hardness (4.5×10^9 N/m²), a high modulus of elasticity around (120 GPa) and a low thermal expansion coefficient (7.5×10^{-9}) and will have a great influence on the mechanical properties of the material (Hao et al., 2021). Mg₂Si phases identified on the welded zone of both samples are surrounded by α -Al (white spots), which contain silicon. It was observed that Mg₂Si phases were bigger on cold rolled sample as compared to as-received sample.

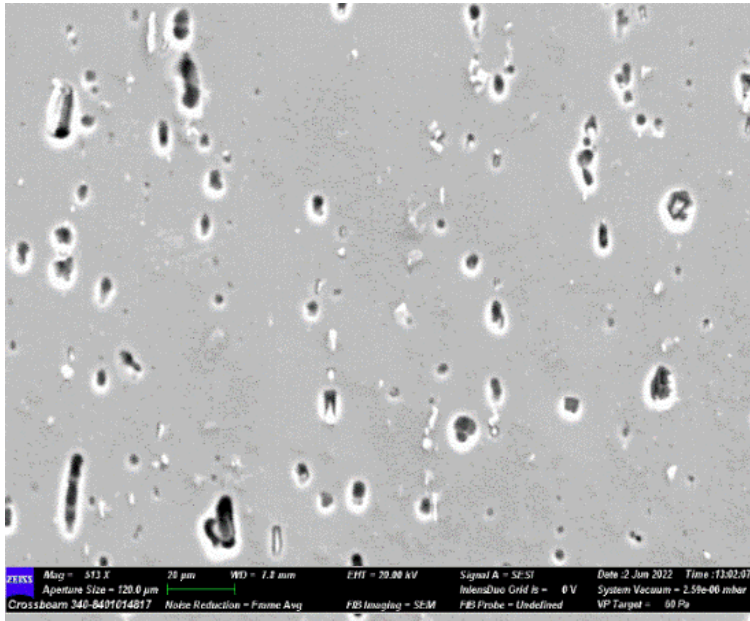


Figure 7: SEM images of as-received material on weld zone.

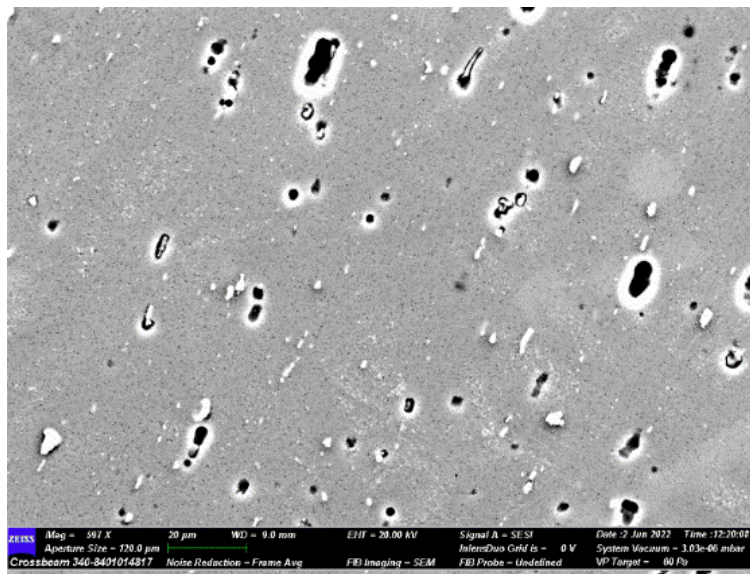


Figure 8: SEM images of cold rolled sample on weld zone

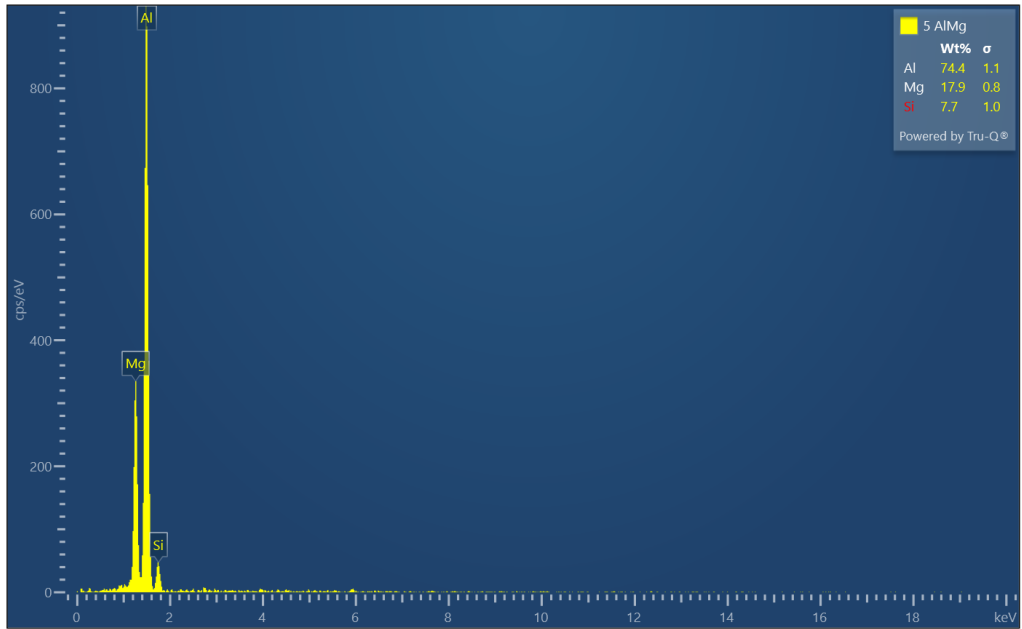


Figure 9: EDS spectrum

Figure 9 presents the EDS spectrum showing Mg₂Si phase on cold-rolled and as-received sample. Mg₂Si was noticed on both materials, but it was varying in compositions Wt% in both materials. It is known that dispersion hardening of the heat-treatable aluminum alloys is based on the precipitation of the metastable precursors of the equilibrium β -Mg₂Si particles (Naumov *et al.*, 2019). The mechanical properties of this friction stir welded alloys are mainly determined by size, volume fraction, and distribution of the precipitates in different weld zones (Naumov *et al.*, 2019) as it is on cold rolled and as-received FSW welded materials in this study.

3.1 Tensile test results

Figure 10 (a-b) illustrates graphically tensile results obtained in table 2.

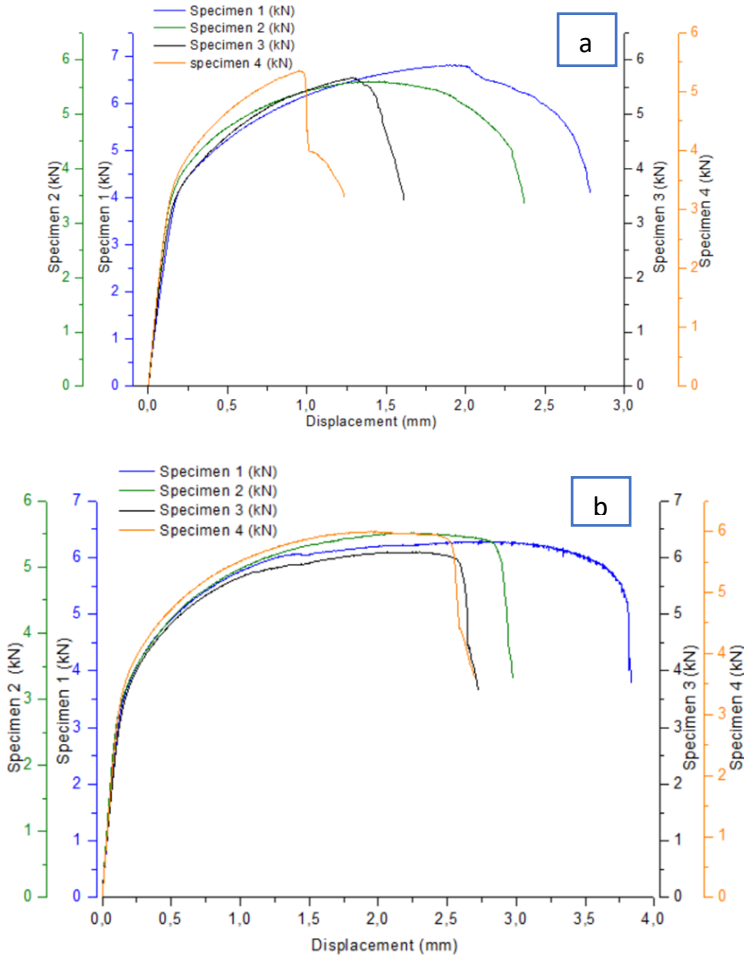


Figure 10 (a-b): Force-displacement curves of (a)As-received FSW welded samples (b) Cold rolled FSW welded material.

Figure 10(a-b) presents the tensile results of as-received and cold-rolled samples. From figure 10a and 10b it was noticed that the materials had similar maximum force. The percentage elongation of rolled welded samples was higher than that of as-received material by 34.9%. The tensile strength of the as-received welded sample was 1.7% more than the cold-rolled sample. There was not much difference in modulus of elasticity of both materials as rolled welded sample is higher by 3.84%. In aluminum alloys, the mechanical properties are seriously diminished by the effect of heat introduced by the welding process(Cueca et al., 2012).

FSW can improve mechanical properties such as fracture toughness, fatigue, and ductility (Hao et al., 2021) .Looking at the fracture mode of four samples of cold reduced material highlighted in figure 4b shows that the material is more ductile as compared to as-received material and this justifies why there is less decrease in mechanical properties on it as compared to as-received FSW welded material. Some of the deviations that might have influence in the results of tensile tests are hooking defects which is one of the most common defects observed in FSW lap joints, which results in a decrease of mechanical properties in the weld when found in the load path(Gungor et al., 2014) to the material used in this study.

From figure 11a hooking defects are identified on as-received material. The hook refers to the last visible point of the interface between joint plates into the stir zone, becoming a geometrical defect that affects the integrity of spot welds because cracks can propagate along it when the weld is subjected to external loading (Piccini and Svoboda, 2015). In figure 11b the hooking defects and tunnelling are identified in cold rolled material. Appropriate material flow is the main reason for defects during FSW, especially for aluminum alloys (Baratzadeh et al., 2020). The same welding parameter were used for both materials and material flow during friction stir welding process would not be the same for both materials because the other material was cold rolled. The tunneling defect occurs when the material flow around the tool pin is inadequate, resulting in an irregular weld filling (Balos and Sidjanin, 2014) as it has been shown on cold rolled material.

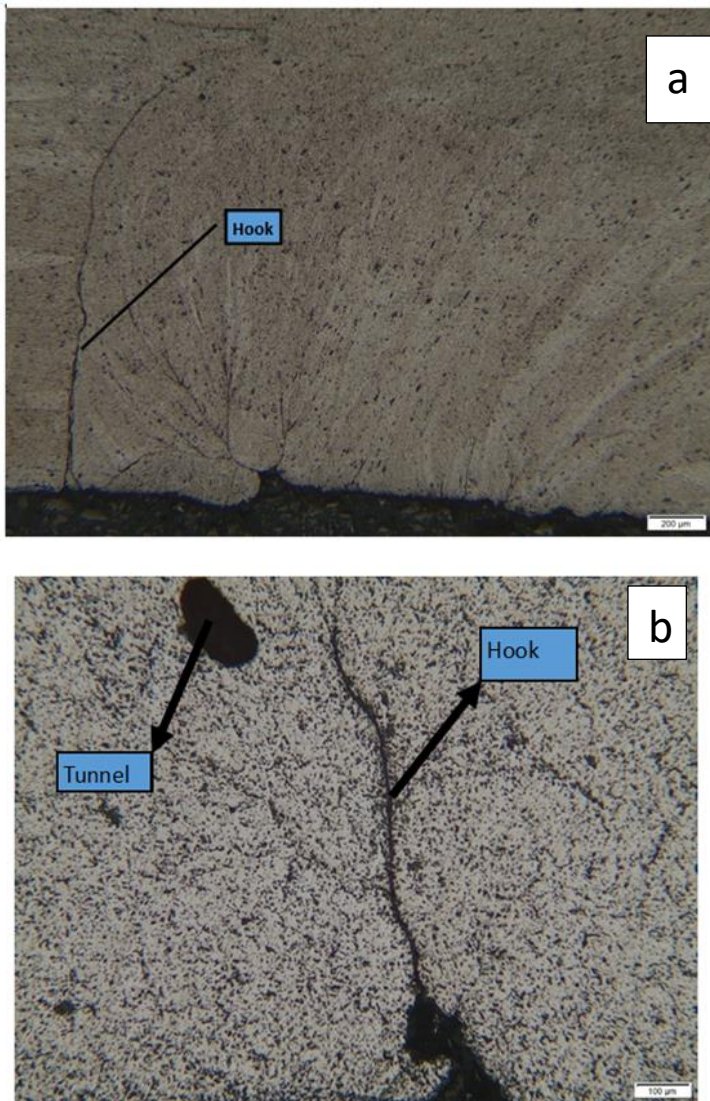


Figure 11 (a-b): (a) Hooking defects of as-received sample (b) Hooking and tunnelling defects of cold rolled sample.

3.2 Hardness test results

The hardness test results which are shown in table 3, are graphically presented in figure 12.

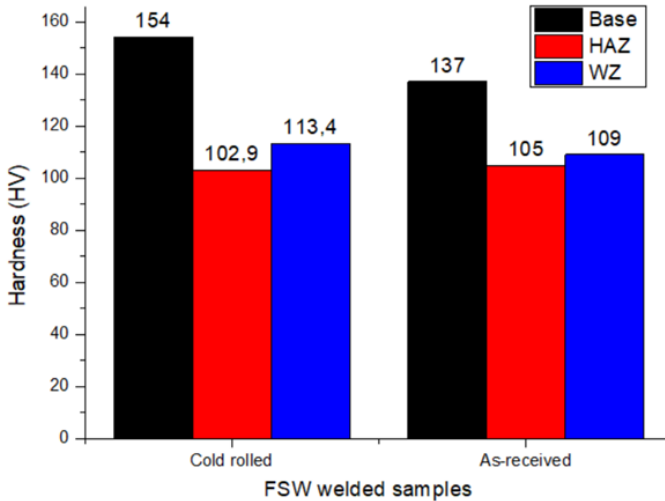


Figure 12: hardness results of cold rolled and as-received samples.

Figure 12 illustrates the hardness results of cold-rolled and as-received welded samples. It was noticed that the cold-rolled sample was 11% harder than the as-received sample on the base metal zone and was reported to be 154 HV. This shows that cold rolling increased the material hardness. The rolling process decreased the material particle sizes. The smaller the particle size, the higher the mechanical properties (hardness). The same results were found in the study of the effect of surface temperature and particle size on mechanical properties during accumulative roll bonding of Al 1050-H4 aluminium alloy (Pita, Mashinini and Tartibu, 2020). It was observed that the decrease in particle sizes achieved by ARB in the first pass increased their hardness. The cold-rolled sample was 4% harder than the as-received sample on WZ. Many of important mechanical properties of materials, including yield strength, hardness and toughness can be improved by refining the grain size(Reza, Ashtiani and Karami, 2015). As-received sample was reported to be harder by 2% as compared to cold rolled welded sample on HAZ. This shows that welding temperature negatively affect the cold rolled sample in this section. In the HAZ, there may be slightly grain growth but there is no plastic deformation(Gungor et al., 2014).

4. Conclusion

The effect of cold rolling on mechanical properties and microstructure of aluminum 6082 T651 joint by friction stir welding process was successfully investigated. The following results were found:

- Rolling process reduced the material thickness by 50% for the purpose of enhancing the material properties before FSW process.
- Bigger Mg₂Si phases were found on the cold rolled welded sample.
- The percentage elongation of rolled welded samples was higher than that of as-received material by 34.9%.
- The tensile strength of as-received welded sample was 1.7% more than that of cold rolled sample.
- There was not much difference in modulus of elasticity of both materials as rolled welded sample is higher by 3.84%.
- It was noticed that cold rolled sample was 11% more harder than as-received sample on the base metal zone and was reported to be 154 HV.
- Cold rolled sample was 4% harder than as-received sample on WZ.
- It can be concluded that cold rolling before welding did increase the mechanical properties of the material under study. Even though it was not that much.

5. References

- [1]. Balos, S. and Sidjanin, L. (2014) 'Effect of tunneling defects on the joint strength efficiency obtained with FSW', *Materiali in Tehnologije*, 48(4), pp. 491–496.
- [2]. Baratzadeh, F. *et al.* (2020) 'Investigation of mechanical properties of AA6082-T6/AA6063-T6 friction stir lap welds', *Journal of Advanced Joining Processes*, 1(November 2019), p. 100011.
- [3]. Baruah, M. and Borah, A. (2020) 'Processing and precipitation strengthening of 6xxx series aluminium alloys: A review', *International Journal of Materials Science*, 1(1), pp. 40–48.
- [4]. Behaviour, S. *et al.* (2020) 'Cold-Rolling Strain Hardening Effect on the Microstructure, Serration-Flow Behaviour and Dislocation Density of Friction Stir Welded AA5083', *metals*.
- [5]. Cueva, F. *et al.* (2012) 'Study of the weld ability of aluminum alloy 5083 H116 with pulsed arc GMAW (GMAW-P)', *Ciencia y tecnología de buques*, 6(11), p. 43.
- [6]. Dong, P. *et al.* (2013) 'Effects of welding speed on the microstructure and hardness in friction stir welding joints of 6005A-T6 aluminum alloy', *JOURNAL OF MATERIALS&DESIGN*, 45, pp. 524–531.
- [7]. Ghalehandi, S. M. and Malaki, M. (2019) *applied sciences Accumulative Roll Bonding — A Review*.
- [8]. Gungor, B. *et al.* (2014) 'Mechanical, fatigue and microstructural properties of friction stir welded 5083-H111 and 6082-T651 aluminum alloys', *Materials and Design*, 56, pp. 84–90.
- [9]. Hao, J. *et al.* (2021) 'Calculation based on the formation of mg₂ si and its effect on the microstructure and properties of al–si alloys', *Materials*, 14(21).
- [10]. Kalinenko, A. *et al.* (2021) 'Materials Science & Engineering A Relationship between welding conditions , abnormal grain growth and mechanical performance in friction-stir welded 6061-T6 aluminum alloy', 817(April).
- [11]. Kawasaki, M. and Langdon, T. G. (2018) 'Fabrication of High Strength Hybrid Materials through the Application of High-Pressure Torsion', 134(3).

- [12]. Kim, H. S. *et al.* (2004) ‘Process Modelling of Equal Channel Angular Pressing for Ultrafine Grained Materials’, 45(7), pp. 2172–2176.
- [13]. Kurzydłowski, K. J. (2004) ‘Microstructural refinement and properties of metals processed by severe plastic deformation’, 52(4), pp. 301–311.
- [14]. Laska, A. *et al.* (2022) ‘Resistance of Friction Stir-Welded AA6082’, pp. 1–16.
- [15]. M. S. Mahany, Reham Reda Abbas, M.M.Z. Ahmed, A. (2017) ‘Influence of Tool Rotational Speed and Axial Load in Friction Stir Welding (Fsw) of High Strength Aluminum Alloys’, *International Journal of Research in Engineering and Technology*, 06(02), pp. 114–120.
- [16]. Naumov, A. *et al.* (2019) ‘Metallurgical and mechanical characterization of high-speed friction stir welded AA 6082-T6 aluminum alloy’, *Materials*, 12(24).
- [17]. Nginda, S. and Pita, M. (2022) ‘Investigation of the Mechanical Properties of Aluminum AA4007 Joints Using the MIG and FSW Processes’, *2022 IEEE 13th International Conference on Mechanical and Intelligent Manufacturing Technologies, ICMIMT 2022*, pp. 11–14.
- [18]. Ortiz, D. *et al.* (2007) ‘Effect of cold work on the tensile properties of 6061, 2024, and 7075 Al alloys’, *Journal of Materials Engineering and Performance*, 16(5), pp. 515–520.
- [19]. Piccini, J. M. and Svoboda, H. G. (2015) ‘Effect of the Tool Penetration Depth in Friction Stir Spot Welding (FSSW) of Dissimilar Aluminum Alloys’, *Procedia Materials Science*, 8, pp. 868–877.
- [20]. Pita, M, P.M Mashinini, L. . T. (2020) ‘The effect of surface temperature and particle size on mechanical properties during accumulative roll bonding of Al 1050-H4 aluminum alloy’, pp. 13–17.
- [21]. Pita, M., Mashinini, P. M. and Tartibu, L. K. (2020) ‘Enhancing of aluminum alloy 1050-H4 tensile strength by accumulative roll bonding process’, *Proceedings of 2020 IEEE 11th International Conference on Mechanical and Intelligent Manufacturing Technologies, ICMIMT 2020*, pp. 31–35.
- [22]. Qassab, R. M. Al and Qassab, R. M. Al (2017) *Effect of Cold Work on Tensile Properties During Annealing Process for Pure Commercial Aluminum (AA 1070 Alloy) Effect of Cold Work on Tensile Properties During Annealing Process for Pure Commercial Aluminum (AA 1070 Alloy)*.
- [23]. Sun, Y. *et al.* (2009) ‘Effect of initial grain size on the joint properties of friction stir welded aluminum’, *Materials Science and Engineering A*, 527(1–2), pp. 317–321.
- [24]. Valiev, R. Z., Islamgaliev, R. K. and Alexandrov, I. V (2000) *Bulk nanostructured materials from severe plastic deformation*.
- [25]. Wang, T. *et al.* (2021) ‘Microstructure and mechanical properties of powder metallurgy 2024 aluminum alloy during cold rolling’, *Journal of Materials Research and Technology*, 15, pp. 3337–3348.
- [26]. Yu, P., Wu, C. and Shi, L. (2021) ‘Acta Materialia Analysis and characterization of dynamic recrystallization and grain structure evolution in friction stir welding of aluminum plates’, 207.
- [27]. Zhu, X. *et al.* (2019) ‘The effects of varying Mg and Si levels on the microstructural inhomogeneity and eutectic Mg₂Si morphology in die-cast Al–Mg–Si alloys’, *Journal of Materials Science*, 54(7), pp. 5773–5787.